Muon Collider:
Probing Anomalous Quartic Gauge Couplings

Yu-Chen Guo

Collaboration with Ji-Chong Yang, Tong Li

LNNU & PITT PACC

2nd Annual US Muon Collider Meeting

University of Chicago, Aug, 07, 2025

Where to next?

- **Evidences for physics beyond the Standard Model**
  - Dark matter, Baryon asymmetry, Neutrino masses, Dark energy, ...
  - Hierarchy, Naturalness, Fine tuning problem, ...

- We haven't found any new particles!

  - Build an even larger collider → go to high energy → discover new particles!
  - Do precision measurements → discover new physics indirectly!

Direct and Indirect Searches for BSM

How do we interpret the measurement results?

Model-dependent

SUSY, 2HDM…

New particles

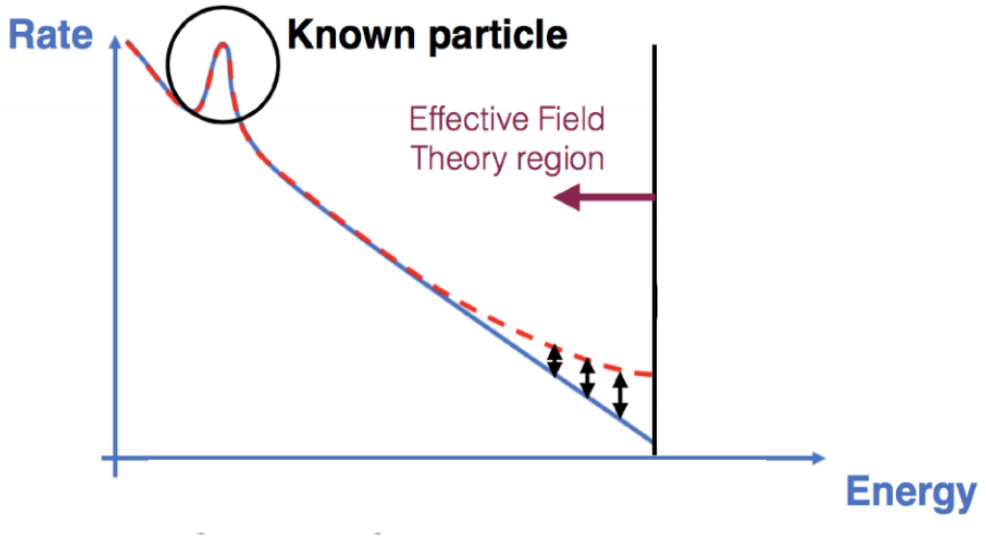

Deviations in tails

Direct and Indirect Searches for BSM

How do we interpret the measurement results?

Model-dependent

SUSY, 2HDM…

New particles

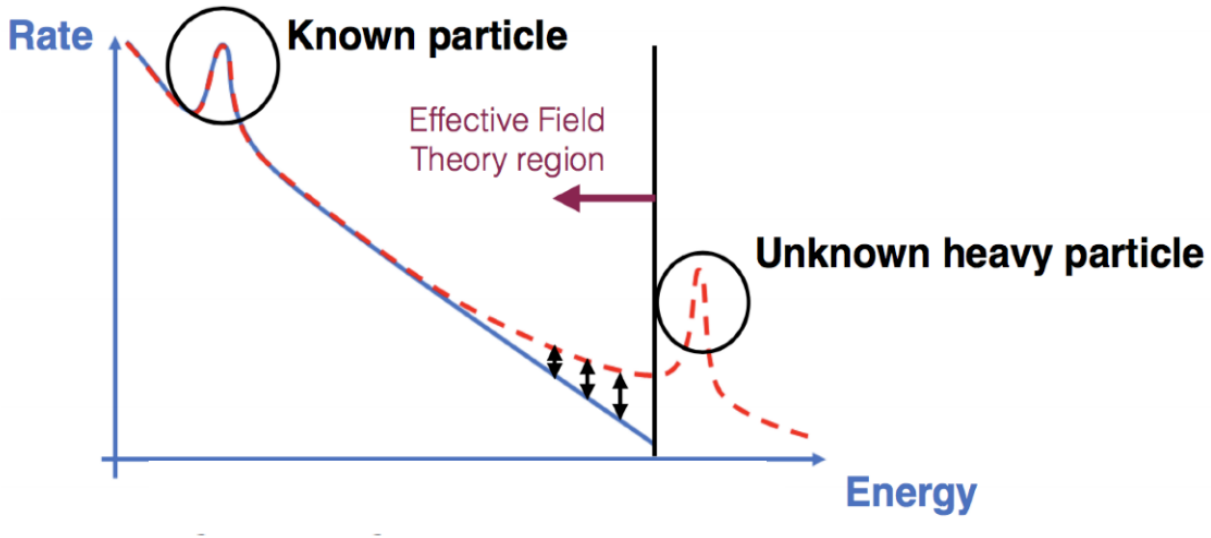

Model-Independent

Simplified models, EFT

New Interactions of SM particles

anomalous couplings

Deviations in tails

Multiboson as a key tool

Rich Results from Multiboson Measurements

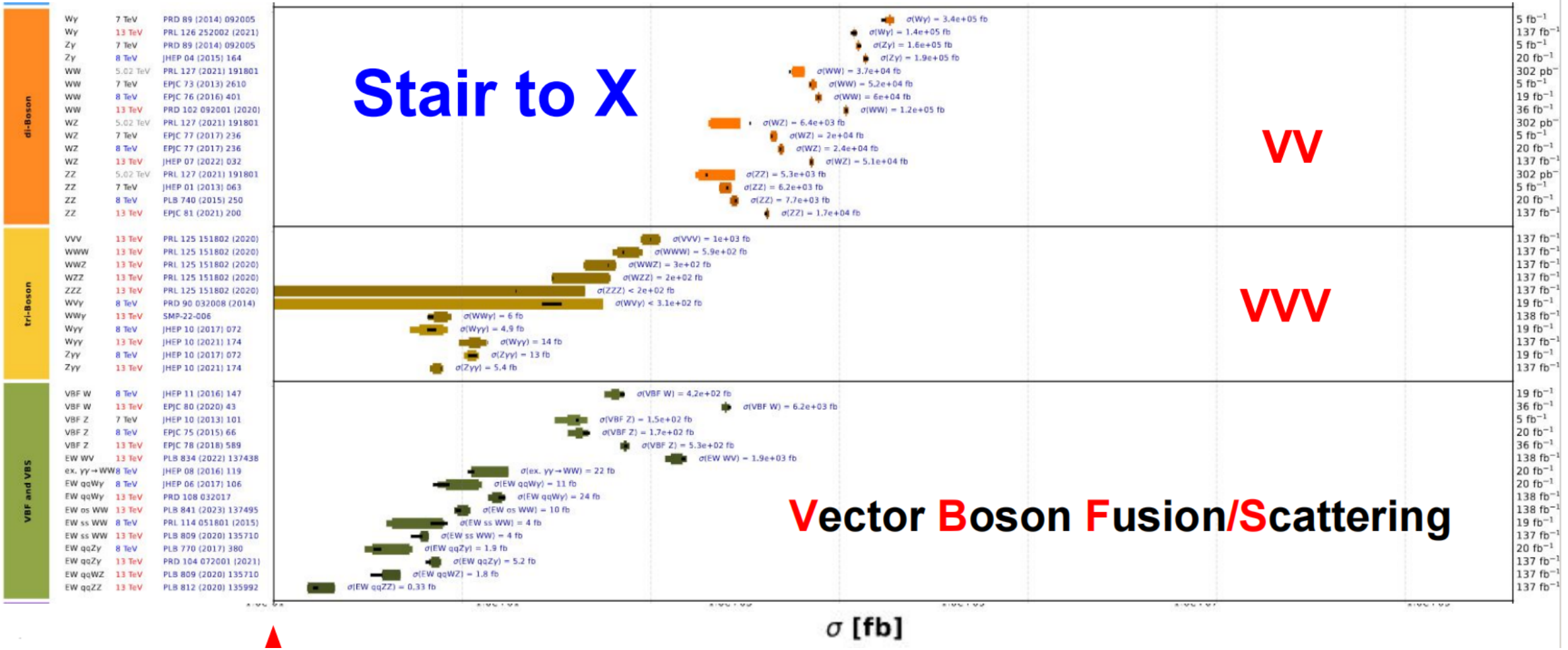

The LHC can also be seen as a Large Boson Collider

MuC: Great Potential to explore unknown

High energy.

High multiplicity.

High opportunities ?

opportunities for both theorists (T) & experimentalists (E)

- ✓ high multiplicity processes
  (T: amplitudes, MC ; E: trackers, machine learning)
- ✓ Transverse vs Longitudinal vectors
  (T: massive amplitudes E: reconstruction)
- ✓ optimizing search analyses
- ✓ global fit

Machines beyond LHC → more energy → better sensitivity

MuC: The large boson-boson collider

Towards a muon collider, EPJC (2023) [2303.08533]

The Standard Model Effective Field Theory

EFT: Bottom-Up approach with general parameterization

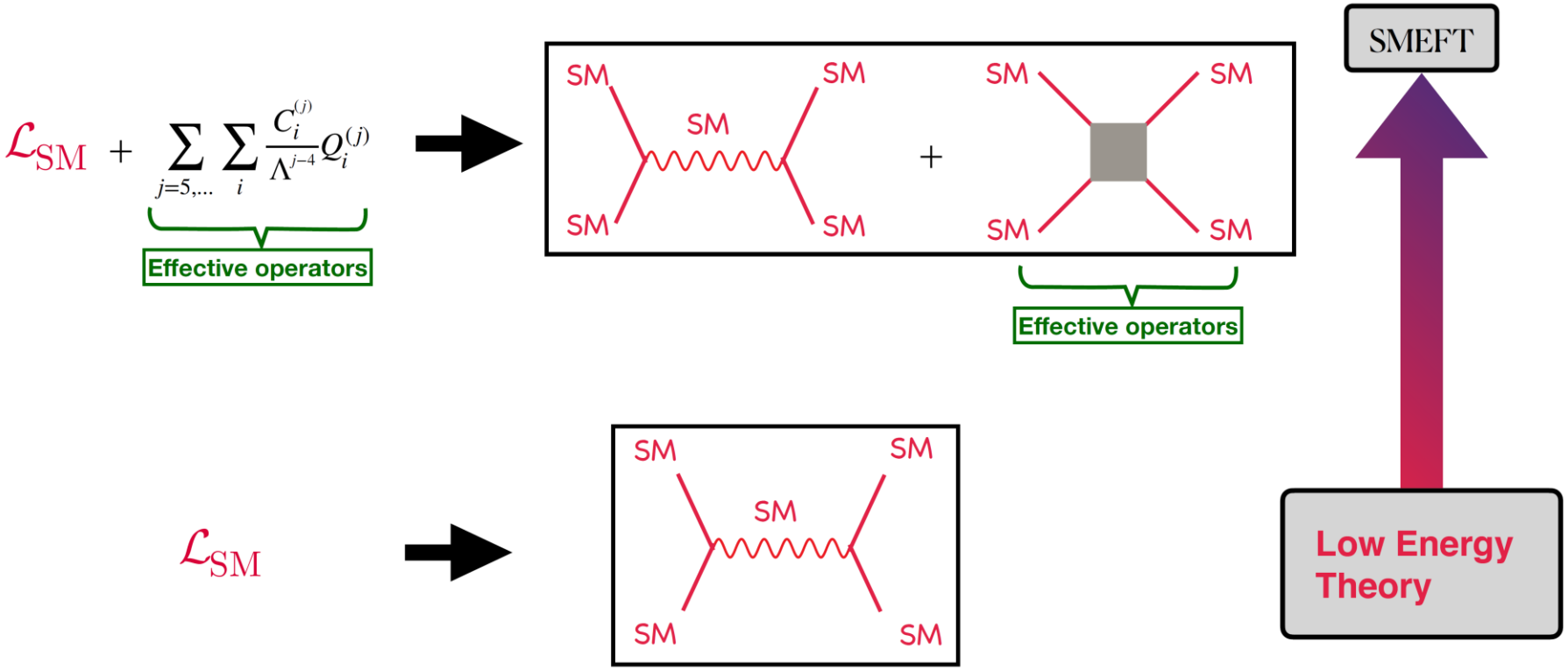

Dimension-8 Operators

- anomalous Quartic Gauge Couplings (aQGC)

$$\mathcal{L}_{\text{SMEFT}} = \mathcal{L}_{SM} + \sum_i \frac{C_{6i}}{\Lambda^2}\mathcal{O}_{6i} + \sum_j \frac{C_{8j}}{\Lambda^4}\mathcal{O}_{8j} + \dots$$

$$\mathcal{L}_{aQGC} = \sum_{i=0}^{2} \frac{f_{S_i}}{\Lambda^4} O_{S_i} + \sum_{j=0}^{7} \frac{f_{M_j}}{\Lambda^4} O_{M_j} + \sum_{k=0}^{9} \frac{f_{T_k}}{\Lambda^4} O_{T_k}$$

$$O_{S_0} = \left[(D_\mu\Phi)^\dagger D_\nu\Phi\right] \times \left[(D^\mu\Phi)^\dagger D^\nu\Phi\right],$$
$$O_{S_1} = \left[(D_\mu\Phi)^\dagger D_\mu\Phi\right] \times \left[(D^\nu\Phi)^\dagger D^\nu\Phi\right],$$
$$O_{S_2} = \left[(D_\mu\Phi)^\dagger D_\nu\Phi\right] \times \left[(D^\nu\Phi)^\dagger D^\mu\Phi\right],$$

$$O_{T_0} = \mathrm{Tr}\left[\widehat{W}_{\mu\nu}\widehat{W}^{\mu\nu}\right] \times \mathrm{Tr}\left[\widehat{W}_{\alpha\beta}\widehat{W}^{\alpha\beta}\right],$$
$$O_{T_1} = \mathrm{Tr}\left[\widehat{W}_{\alpha\nu}\widehat{W}^{\mu\beta}\right] \times \mathrm{Tr}\left[\widehat{W}_{\mu\beta}\widehat{W}^{\alpha\nu}\right],$$
$$O_{T_2} = \mathrm{Tr}\left[\widehat{W}_{\alpha\mu}\widehat{W}^{\mu\beta}\right] \times \mathrm{Tr}\left[\widehat{W}_{\beta\nu}\widehat{W}^{\nu\alpha}\right],$$
$$O_{T_5} = \mathrm{Tr}\left[\widehat{W}_{\mu\nu}\widehat{W}^{\mu\nu}\right] \times B_{\alpha\beta}B^{\alpha\beta},$$
$$O_{T_6} = \mathrm{Tr}\left[\widehat{W}_{\alpha\nu}\widehat{W}^{\mu\beta}\right] \times B_{\mu\beta}B^{\alpha\nu},$$
$$O_{T_7} = \mathrm{Tr}\left[\widehat{W}_{\alpha\mu}\widehat{W}^{\mu\beta}\right] \times B_{\beta\nu}B^{\nu\alpha},$$
$$O_{T_8} = B_{\mu\nu}B^{\mu\nu} \times B_{\alpha\beta}B^{\alpha\beta},$$
$$O_{T_9} = B_{\alpha\mu}B^{\mu\beta} \times B_{\beta\nu}B^{\nu\alpha},$$

$$O_{M_0} = \mathrm{Tr}\left[\widehat{\mathrm{W}}_{\mu\nu}\widehat{\mathrm{W}}^{\mu\nu}\right] \times \left[(D^\beta\Phi)^\dagger D^\beta\Phi\right],$$
$$O_{M_1} = \mathrm{Tr}\left[\widehat{\mathrm{W}}_{\mu\nu}\widehat{\mathrm{W}}^{\nu\beta}\right] \times \left[(D^\beta\Phi)^\dagger D^\mu\Phi\right],$$
$$O_{M_2} = \left[B_{\mu\nu}B^{\mu\nu}\right] \times \left[(D^\beta\Phi)^\dagger D^\beta\Phi\right],$$
$$O_{M_3} = \left[B_{\mu\nu}B^{\nu\beta}\right] \times \left[(D^\beta\Phi)^\dagger D^\mu\Phi\right],$$
$$O_{M_4} = \left[(D_\mu\Phi)^\dagger \widehat{W}_{\beta\nu}D^\mu\Phi\right] \times B^{\beta\nu},$$
$$O_{M_5} = \left[(D_\mu\Phi)^\dagger \widehat{W}_{\beta\nu}D_\nu\Phi\right] \times B^{\beta\mu} + h.c.,$$
$$O_{M_7} = (D_\mu\Phi)^\dagger \widehat{W}_{\beta\nu}\widehat{W}_{\beta\mu}D_\nu\Phi,$$

Eboli, Gonzalez-Garcia, Mizukoshi, PRD (2006) [hep-ph/0606118]

Eboli, Gonzalez-Garcia, PRD (2016) [1604.03555]

Dimension-8 Operators

- gluonic Quartic Gauge Couplings (gQGC)

$$\mathcal{L}_{\text{SMEFT}} = \mathcal{L}_{SM} + \sum_i \frac{C_{6i}}{\Lambda^2}\mathcal{O}_{6i} + \sum_j \frac{C_{8j}}{\Lambda^4}\mathcal{O}_{8j} + \dots$$

$$\begin{aligned}
\mathcal{O}_{gT,0} &\equiv \sum_a G^a_{\mu\nu}G^{a,\mu\nu} \times \sum_i W^i_{\alpha\beta}W^{i,\alpha\beta}\,,\\
\mathcal{O}_{gT,1} &\equiv \sum_a G^a_{\alpha\nu}G^{a,\mu\beta} \times \sum_i W^i_{\mu\beta}W^{i,\alpha\nu}\,,\\
\mathcal{O}_{gT,2} &\equiv \sum_a G^a_{\alpha\mu}G^{a,\mu\beta} \times \sum_i W^i_{\nu\beta}W^{i,\alpha\nu}\,,\\
\mathcal{O}_{gT,3} &\equiv \sum_a G^a_{\alpha\mu}G^a_{\beta\nu} \times \sum_i W^{i,\mu\beta}W^{i,\nu\alpha}\,,\\
\mathcal{O}_{gT,4} &\equiv \sum_a G^a_{\mu\nu}G^{a,\mu\nu} \times B_{\alpha\beta}B^{\alpha\beta}\,,\\
\mathcal{O}_{gT,5} &\equiv \sum_a G^a_{\alpha\nu}G^{a,\mu\beta} \times B_{\mu\beta}B^{\alpha\nu}\,,\\
\mathcal{O}_{gT,6} &\equiv \sum_a G^a_{\alpha\mu}G^{a,\mu\beta} \times B_{\nu\beta}B^{\alpha\nu}\,,\\
\mathcal{O}_{gT,7} &\equiv \sum_a G^a_{\alpha\mu}G^a_{\beta\nu} \times B^{\mu\beta}B^{\nu\alpha}\,,
\end{aligned}$$

$$\mathcal{L}_{aQGC} = \sum_{i=0}^{2}\frac{f_{S_i}}{\Lambda^4}O_{S_i} + \sum_{j=0}^{7}\frac{f_{M_j}}{\Lambda^4}O_{M_j} + \sum_{k=0}^{9}\frac{f_{T_k}}{\Lambda^4}O_{T_k}$$

"The gluonic QGC is a natural extension of QED Born-Infeld theory, supported by String Theory"

Ellis, Ge. PRL (2018) [1802.02416]

$$\mathcal{L}_{gT} = \sum_{i=0}^{7}\frac{1}{16M_i^4}\mathcal{O}_{gT,i}$$

Born-Infeld Extensions

$$\beta^2\left[1-\sqrt{1+\sum_{\lambda=1}^{12}\frac{F^\lambda_{\mu\nu}F^{\lambda,\mu\nu}}{2\beta^2}-\left(\sum_{\lambda=1}^{12}\frac{F^\lambda_{\mu\nu}\widetilde{F}^{\lambda,\mu\nu}}{4\beta^2}\right)^2}\right]$$

$$\approx -\frac{1}{4}\sum_{\lambda=1}^{12}F^\lambda_{\mu\nu}F^{\lambda,\mu\nu} + \frac{1}{32\beta^2}\left[\left(\sum_{\lambda=1}^{12}F^\lambda_{\mu\nu}F^{\lambda,\mu\nu}\right)^2 + \left(\sum_{\lambda=1}^{12}F^\lambda_{\mu\nu}\widetilde{F}^{\lambda,\mu\nu}\right)^2\right] \equiv \mathcal{L}_{\text{SM}} + \mathcal{L}_{\text{gT}}$$

with a single parameter $\beta \equiv M^2$ & $\mathcal{L}_{\text{gT}} = \sum_{i=0}^{7}\frac{1}{16\beta_i^2}\mathcal{O}_{\text{gT,i}}$

Multi-boson physics studies at MuC

anomalous Quartic Gauge Couplings （ aQGC ）

- VBS (AA+$\not{E}$) : $\mu^+\mu^- \to \gamma\gamma\nu\bar{\nu}$
- VBS (WW+$\not{E}$): $\mu^+\mu^- \to W^+W^-\nu\bar{\nu}$
- Triboson (AAA): $\mu^+\mu^- \to \gamma\gamma\gamma$

gluonic Quartic Gauge Couplings （ gQGC ）

- Triboson (AGG): $\mu^+\mu^- \to \gamma jj$

aQGC: VBS (AA+$\not{E}$)

- aQGC in the VBS of $W^+W^- \to \gamma\gamma$ ($\gamma\gamma\nu\bar{\nu}$)

Y-C G, Feng & Yang, to be uploaded to arXiv

aQGC:

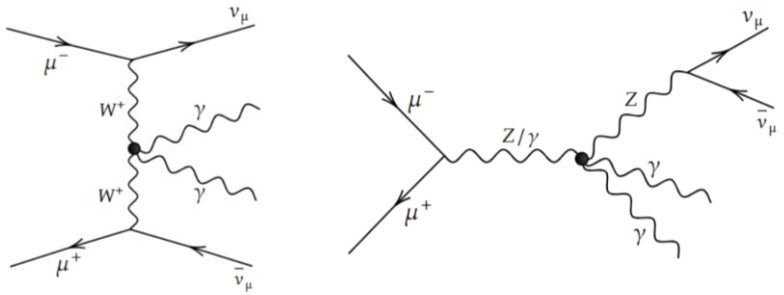

SM :

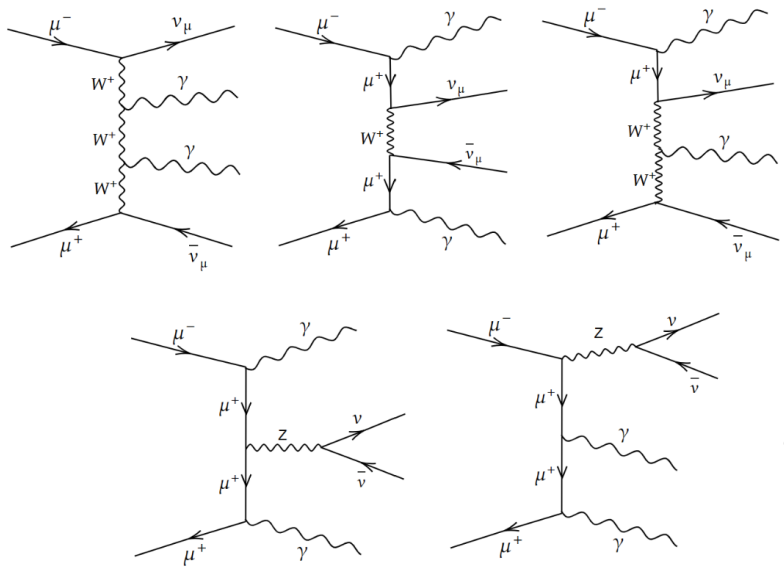

...

Comparison of **VBS** and **Tri-boson**

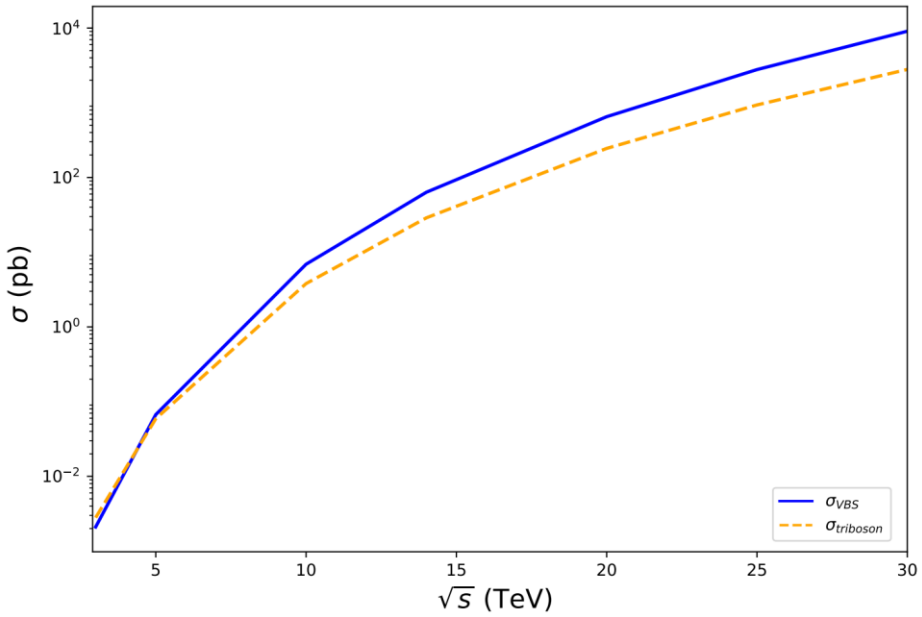

When a new particle X is produced, there is a relative scaling

$$\frac{\sigma_{\mathrm{VBF}}^{\mathrm{BSM}}}{\sigma_{\mathrm{ann}}^{\mathrm{BSM}}} \propto \alpha_W^2 \frac{s}{m_X^2} \log^2\left(\frac{s}{m_V^2}\right) \log\left(\frac{s}{m_X^2}\right)$$

Al Ali et al., RPP (2022) [2103.14043]

aQGC: VBS (AA+$\not{E}$)

- aQGC in the VBS of $W^+W^-\to\gamma\gamma$ ($\gamma\gamma\nu\bar{\nu}$)

Y-C G, Feng & Yang, to be uploaded to arXiv

Partial-wave Unitary

$$\mathcal{M}(V_{1\lambda_1}V_{2\lambda_2}\to V_{3\lambda_3}V_{4\lambda_4}) = 16\pi\sum_J (J+\frac{1}{2})\sqrt{1+\delta_{V_{1\lambda_1}}^{V_{2\lambda_2}}}\sqrt{1+\delta_{V_{3\lambda_3}}^{V_{4\lambda_4}}}\, d^J_{\lambda\mu}(\theta,\varphi)\, e^{iM\varphi} \times T^J(V_{1\lambda_1}V_{2\lambda_2}\to V_{3\lambda_3}V_{4\lambda_4})$$

Unitary bounds for VBS process of $W^+W^-\to\gamma\gamma$

$$\left|\frac{f_{M_0}}{\Lambda^4}\right| \le \frac{128\sqrt{2}\pi M_W^2}{e^2v^2\hat{s}^2}, \quad \left|\frac{f_{M_1}}{\Lambda^4}\right| \le \frac{512\sqrt{2}\pi M_W^2}{e^2v^2\hat{s}^2}, \quad \left|\frac{f_{M_2}}{\Lambda^4}\right| \le \frac{64\sqrt{2}\pi M_W^2 s_W^2}{c_W^2 e^2v^2\hat{s}^2},$$
$$\left|\frac{f_{M_3}}{\Lambda^4}\right| \le \frac{256\sqrt{2}\pi M_W^2 s_W^2}{c_W^2 e^2v^2\hat{s}^2}, \quad \left|\frac{f_{M_4}}{\Lambda^4}\right| \le \frac{128\sqrt{2}\pi M_W^2 s_W}{c_W e^2v^2\hat{s}^2}, \quad \left|\frac{f_{M_5}}{\Lambda^4}\right| \le \frac{256\sqrt{2}\pi M_W^2 s_W}{c_W e^2v^2\hat{s}^2},$$
$$\left|\frac{f_{M_7}}{\Lambda^4}\right| \le \frac{1024\sqrt{2}\pi M_W^2}{e^2v^2\hat{s}^2},$$
$$\left|\frac{f_{T_0}}{\Lambda^4}\right| \le \frac{8\sqrt{2}\pi}{s_W^2\hat{s}^2}, \quad \left|\frac{f_{T_1}}{\Lambda^4}\right| \le \frac{24\sqrt{2}\pi}{s_W^2\hat{s}^2}, \quad \left|\frac{f_{T_2}}{\Lambda^4}\right| \le \frac{32\sqrt{2}\pi}{s_W^2\hat{s}^2},$$
$$\left|\frac{f_{T_5}}{\Lambda^4}\right| \le \frac{8\sqrt{2}\pi}{c_W^2\hat{s}^2}, \quad \left|\frac{f_{T_6}}{\Lambda^4}\right| \le \frac{24\sqrt{2}\pi}{c_W^2\hat{s}^2}, \quad \left|\frac{f_{T_7}}{\Lambda^4}\right| \le \frac{32\sqrt{2}\pi}{c_W^2\hat{s}^2},$$

	($\sqrt{s}=3$ TeV)	($\sqrt{s}=14$ TeV)	($\sqrt{s}=30$ TeV)
f_{M_2}/Λ^4 (TeV^{-4})	$[-1.2, 1.2]$	$[-0.0025, 0.0025]$	$[-0.00012, 0.00012]$
f_{M_3}/Λ^4 (TeV^{-4})	$[-4.8, 4.8]$	$[-0.01, 0.01]$	$[-0.00048, 0.00048]$
f_{M_4}/Λ^4 (TeV^{-4})	$[-4.4, 4.4]$	$[-0.0093, 0.0093]$	$[-0.00044, 0.00044]$
f_{T_0}/Λ^4 (TeV^{-4})	$[-1.90, 1.90]$	$[-0.004, 0.004]$	$[-0.00019, 0.00019]$
f_{T_1}/Λ^4 (TeV^{-4})	$[-5.69, 5.69]$	$[-0.012, 0.012]$	$[-0.00057, 0.00057]$
f_{T_2}/Λ^4 (TeV^{-4})	$[-7.59, 7.59]$	$[-0.016, 0.016]$	$[-0.00075, 0.00075]$
f_{T_5}/Λ^4 (TeV^{-4})	$[-0.57, 0.57]$	$[-0.0012, 0.0012]$	$[-0.000057, 0.000057]$
f_{T_6}/Λ^4 (TeV^{-4})	$[-1.71, 1.71]$	$[-0.0036, 0.0036]$	$[-0.00017, 0.00017]$
f_{T_7}/Λ^4 (TeV^{-4})	$[-2.28, 2.28]$	$[-0.0048, 0.0048]$	$[-0.00022, 0.00022]$

aQGC: VBS (AA+$\not{E}$)

Part of the kinematic observables

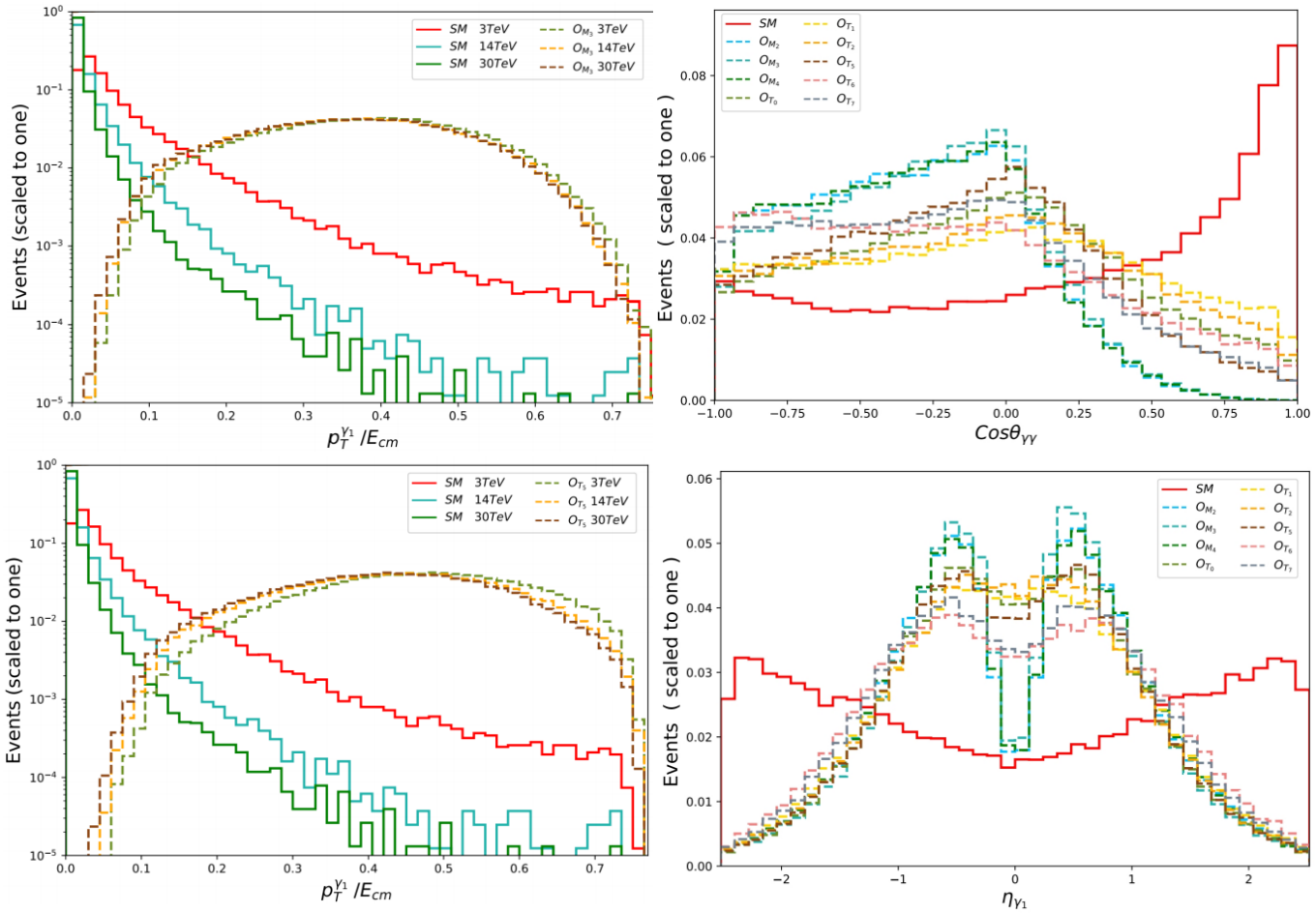

Compare to 13 TeV LHC:
the expected constraints can be improved by 2~3 orders of magnitude for 14 TeV MuC ,
and by 4 orders of magnitude for 30 TeV MuC.

Expected aQGC coefficients

	$\mathcal{S}_{stat}$	3 TeV $1ab^{-1}$	14 TeV $10ab^{-1}$	30 TeV $10ab^{-1}$
$\frac{f_{M_2}}{\Lambda^4}$	2	[-0.892, 0.877]	[-0.00758, 0.00462]	[-0.000335, 0.000338]
	3	[-1.101, 1.086]	[-0.00909, 0.00612]	[-0.000424, 0.000427]
	5	[-1.444, 1.429]	[-0.0118, 0.00881]	[-0.000582, 0.000585]
$\frac{f_{M_3}}{\Lambda^4}$	2	[-2.994, 3.379]	[-0.0199, 0.0271]	[-0.000491, 0.00105]
	3	[-3.742, 4.128]	[-0.0259, 0.0331]	[-0.000669, 0.00123]
	5	[-4.974, 5.360]	[-0.0365, 0.0437]	[-0.000994, 0.00155]
$\frac{f_{M_4}}{\Lambda^4}$	2	[-3.085, 3.312]	[-0.0111, 0.0350]	[-0.000491, 0.00145]
	3	[-3.837, 4.065]	[-0.0157, 0.0395]	[-0.00108, 0.00173]
	5	[-5.077, 5.304]	[-0.0242, 0.0480]	[-0.00157, 0.00223]
$\frac{f_{T_0}}{\Lambda^4}$	2	[-0.248, 0.126]	[-0.000653, 0.000374]	[-0.0000499, 0.0000277]
	3	[-0.288, 0.166]	[-0.000774,0.000496]	[-0.0000592, 0.0000370]
	5	[-0.355, 0.233]	[-0.000989, 0.000710]	[-0.0000758, 0.0000535]
$\frac{f_{T_1}}{\Lambda^4}$	2	[-0.209, 0.142]	[-0.000495, 0.000316]	[-0.0000554, 0.0000290]
	3	[-0.249, 0.182]	[-0.000603, 0.000423]	[-0.0000654, 0.0000390]
	5	[-0.316, 0.248]	[-0.000804, 0.000624]	[-0.0000833, 0.0000570]
$\frac{f_{T_2}}{\Lambda^4}$	2	[-0.561, 0.265]	[-0.00118, 0.000613]	[-0.0000695, 0.0000622]
	3	[-0.647, 0.351]	[-0.00140, 0.000830]	[-0.0000875, 0.0000801]
	5	[-0.791, 0.495]	[-0.00179, 0.00123]	[-0.000120, 0.000113]
$\frac{f_{T_5}}{\Lambda^4}$	2	[-0.115, 0.067]	[-0.000271, 0.000134]	[-0.0000158, 0.0000128]
	3	[-0.135, 0.087]	[-0.000319, 0.000182]	[-0.0000195, 0.0000165]
	5	[-0.168, 0.120]	[-0.000407, 0.000270]	[-0.0000260, 0.0000229]
$\frac{f_{T_6}}{\Lambda^4}$	2	[-0.128, 0.114]	[-0.000202, 0.000149]	[-0.0000385, 0.0000254]
	3	[-0.156, 0.142]	[-0.000254, 0.000201]	[-0.0000462, 0.0000331]
	5	[-0.203, 0.189]	[-0.000356, 0.000302]	[-0.0000595, 0.0000463]
$\frac{f_{T_7}}{\Lambda^4}$	2	[-0.317, 0.189]	[-0.000349, 0.000238]	[-0.0000385, 0.0000395]
	3	[-0.374, 0.245]	[-0.000449,0.000337]	[-0.0000487, 0.0000497]
	5	[-0.467, 0.339]	[-0.000651, 0.000540]	[-0.0000666, 0.0000676]

aQGC: VBS (AA+$\not{E}$)

Machine learning algorithm: nested local outlier factor (NLOF)

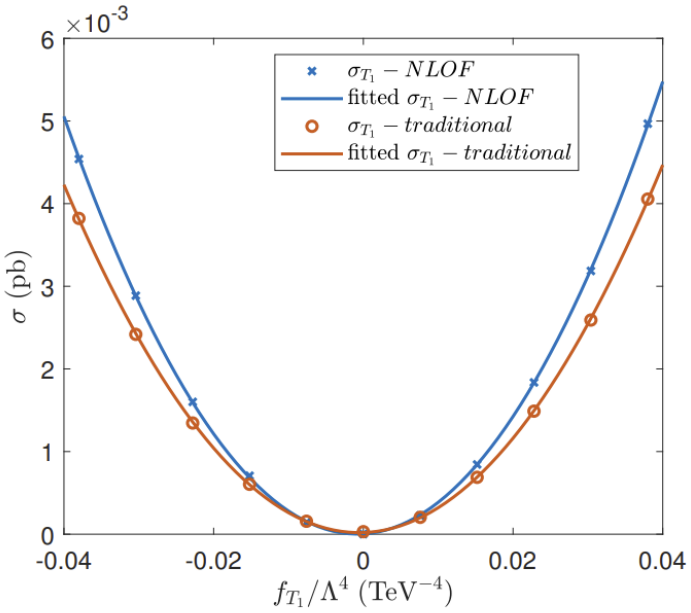

FIG. 5. Comparison of the cross section after cut between the case of a traditional event selection strategy and the NLOF for O_{T_1} at $\sqrt{s} = 10$ TeV.

*Chen, **Y-C G** & Yang, [2504.03145]*

	S_{stat}	3 TeV 1 ab^{-1} (TeV^{-4})		S_{stat}	3 TeV 1 ab^{-1} (TeV^{-4})
$\frac{f_{M_2}}{\Lambda^4}$	2	$[-0.267, 0.284]$	$\frac{f_{M_3}}{\Lambda^4}$	2	$[-0.898, 0.912]$
	3	$[-0.333, 0.349]$		3	$[-1.11, 1.13]$
	5	$[-0.440, 0.457]$		5	$[-1.47, 1.48]$
$\frac{f_{M_4}}{\Lambda^4}$	2	$[-0.845, 0.940]$	$\frac{f_{M_5}}{\Lambda^4}$	2	$[-1.64, 2.07]$
	3	$[-1.06, 1.15]$		3	$[-2.07, 2.51]$
	5	$[-1.41, 1.50]$		5	$[-2.79, 3.22]$
$\frac{f_{T_0}}{\Lambda^4}$	2	$[-0.124, 0.0415]$	$\frac{f_{T_1}}{\Lambda^4}$	2	$[-0.134, 0.0333]$
	3	$[-0.139, 0.0565]$		3	$[-0.147, 0.0464]$
	5	$[-0.165, 0.0825]$		5	$[-0.170, 0.0693]$
$\frac{f_{T_2}}{\Lambda^4}$	2	$[-0.231, 0.0471]$	$\frac{f_{T_5}}{\Lambda^4}$	2	$[-0.0533, 0.0265]$
	3	$[-0.251, 0.0665]$		3	$[-0.0617, 0.0348]$
	5	$[-0.285, 0.101]$		5	$[-0.0756, 0.0487]$
$\frac{f_{T_6}}{\Lambda^4}$	2	$[-0.0620, 0.0261]$	$\frac{f_{T_7}}{\Lambda^4}$	2	$[-0.183, 0.0479]$
	3	$[-0.0708, 0.0348]$		3	$[-0.201, 0.0663]$
	5	$[-0.0855, 0.0496]$		5	$[-0.233, 0.0981]$

As an unsupervised ML algorithm, NLOF can automatically discover the anomalies

aQGC: VBS (WW+$\not{E}$)

The exclusive $W^+W^- \to W^+W^-$ scattering

*Yang, Han, Qin, Li, **Y-C G**, JHEP (2022) [2204.10034]*

Features of this process with purely leptonic decay:

- Absence of QCD background:
  No composite particles in the initial states, so no significant QCD background.
- Initial state of the sub-process known:
  The high-energy muon beams radiate W bosons and turn into neutrinos
  (concentrate on $WWWW$ vertex)

Various processes contribute to the signal

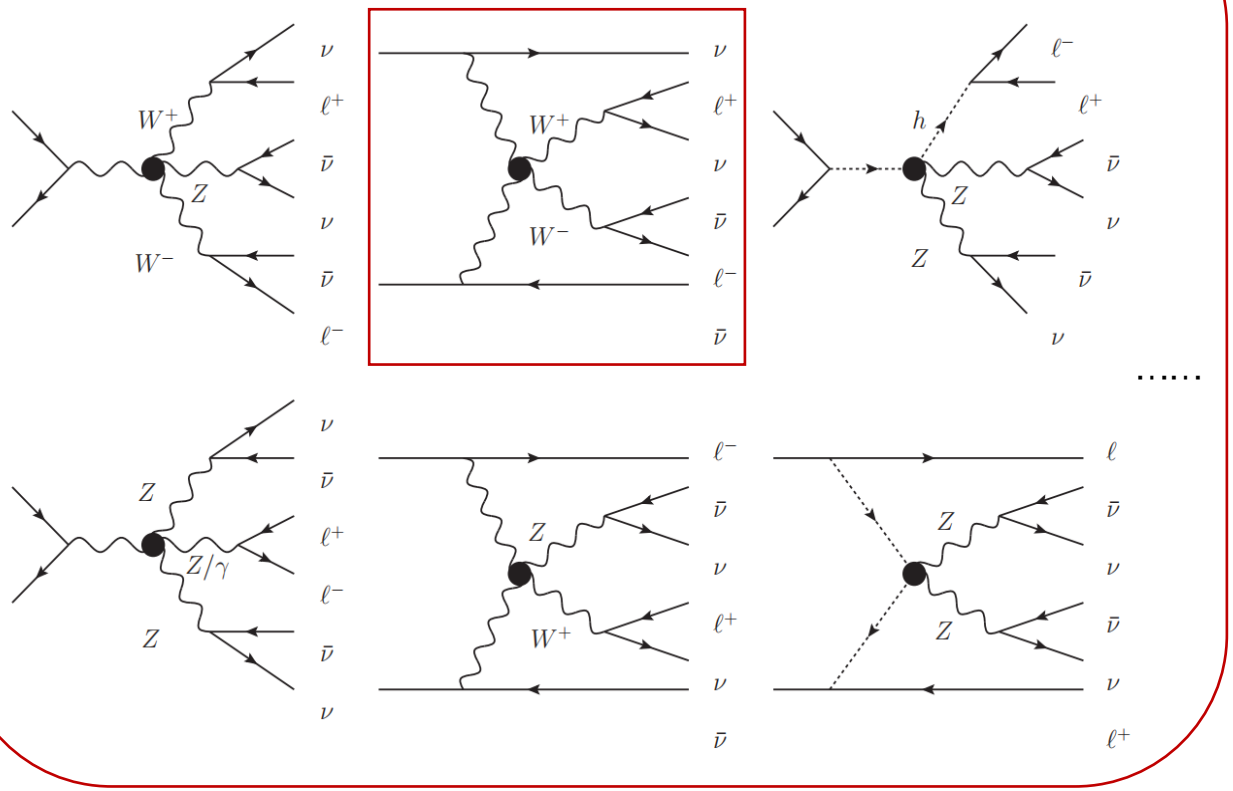

aQGC: VBS (WW+$\not{E}$)

Artificial Neural Networks (ANN)

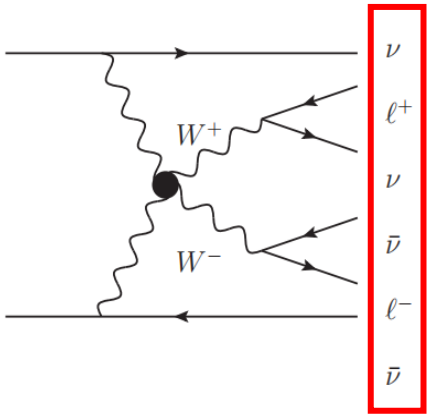

14 Input variables : 14-dimension vector

= 4-momenta of charged leptons & missing momentum
(12 components)
+ the flavors of the charged leptons
(2 components)

1 Output variable: W_{score}

Machine learning can be used for extracting subprocess

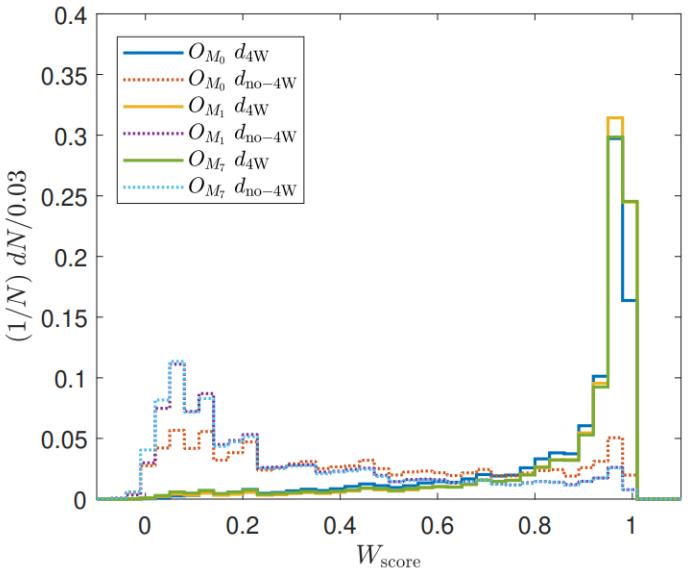

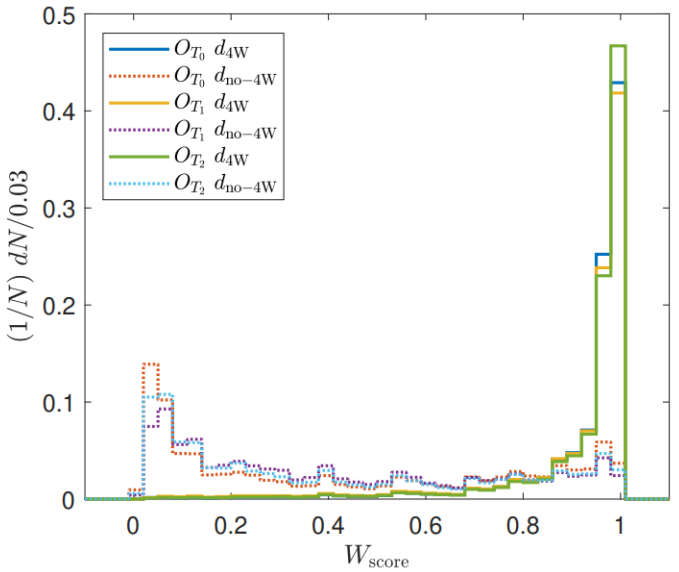

Utilizing an ANN, the W_{score} predicts whether an event is from the $W^{\pm}W^{\pm} \rightarrow W^{\pm}W^{\pm}$ process (1 for yes, 0 for no).

aQGC: VBS (WW+$\not{E}$)

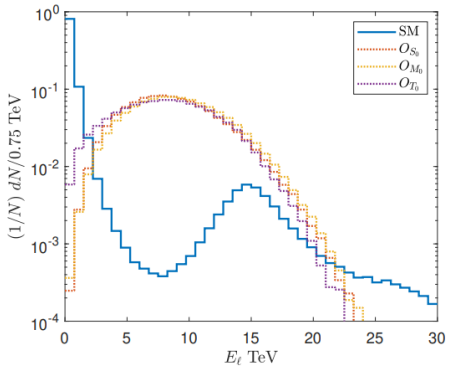

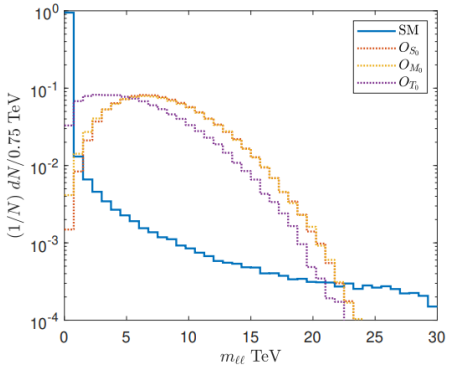

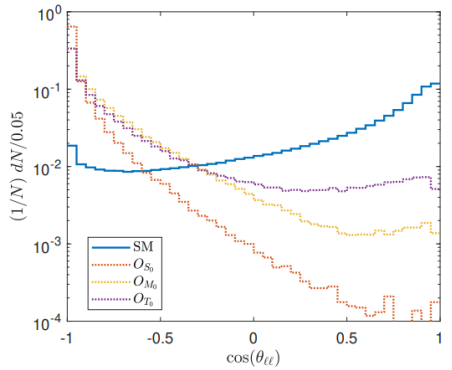

Cross-sections (ab) after cuts at $\sqrt{s} = 30$ TeV.

f_{S_i}/Λ^4	SM	O_{S_0} 0.1	O_{S_1} 0.1	O_{S_2} 0.1
σ	176805	23559	56280	56326
N_ℓ cut	140132	18054	43441	43570
2.2 TeV $< E_\ell <$ 22 TeV	7786.7	17835	42912	43046
2 TeV $< m_{\ell\ell} <$ 20 TeV	4138.8	17594	42331	42460
$\cos(\theta_{\ell\ell}) < -0.3$	2632.3	17378		41758
$\cos(\theta_{\ell\ell}) < -0.8$	1674.8		36049	
f_{M_i}/Λ^4	SM	O_{M_0} 0.002	O_{M_1} 0.004	O_{M_7} 0.008
σ	176805	964.0	714.2	955.5
N_ℓ cut	140132	743.8	548.8	738.0
2.2 TeV $< E_\ell <$ 22 TeV	7786.7	735.9	542.2	728.5
2.2 TeV $< m_{\ell\ell} <$ 20 TeV	3935.0	709.7	516.2	684.7
$W_{\text{score}} > 0.85$	964.9	402.0	273.2	
$W_{\text{score}} > 0.95$	403.8			220.8
f_{T_i}/Λ^4	SM	O_{T_0} 0.0002	O_{T_1} 0.0003	O_{T_2} 0.0005
σ	176805	621.7	944.8	842.8
N_ℓ cut	140132	485.2	726.0	649.4
2.2 TeV $< E_\ell <$ 22 TeV	7786.7	462.2	688.2	603.0
2.8 TeV $< m_{\ell\ell} <$ 18 TeV	3288.0	366.8	553.3	477.1
$W_{\text{score}} > 0.85$	482.0		362.5	346.4
$W_{\text{score}} > 0.9$	299.2	246.2		

Expected constraints on coefficients (absolute value with 10^{-3}TeV^{-4}) at $\sqrt{s} = 30$ TeV and $L = 10$ ab^{-1}. Systematic errors are from results with unitarity bounds by factors ½ and 2.

$\mathcal{S}_{\text{stat}}$	f_{S_0}/Λ^4	f_{S_1}/Λ^4	f_{S_2}/Λ^4
2	$35.3^{+39.5}_{-27.5}$	$61.4^{+21.8}_{-15.6}$	$42.4^{+10.8}_{-0.3}$
3	$72.0^{+20.7}_{-59.5}$	$78.0^{+30.0}_{-5.2}$	$60.0^{+14.6}_{-1.0}$
5	$111.7^{+48.0}_{-87.7}$	$166.3^{+48.6}_{-52.9}$	$95.8^{+12.5}_{-4.3}$
$\mathcal{S}_{\text{stat}}$	f_{M_0}/Λ^4	f_{M_1}/Λ^4	f_{M_7}/Λ^4
2	$0.45^{+0.59}_{-0.01}$	$1.08^{+0.31}_{-0}$	$1.91^{+0.34}_{-0}$
3	$0.59^{+1.28}_{-0.05}$	$1.35^{+1.07}_{-0.03}$	$2.37^{+1.31}_{-0}$
5	$0.99^{+4.15}_{-0.29}$	$1.90^{+3.88}_{-0.19}$	$3.23^{+8.92}_{-0.15}$
$\mathcal{S}_{\text{stat}}$	f_{T_0}/Λ^4	f_{T_1}/Λ^4	f_{T_2}/Λ^4
2	$0.043^{+0.006}_{-0}$	$0.059^{+0.010}_{-0.001}$	$0.101^{+0.012}_{-0}$
3	$0.053^{+0.014}_{-0}$	$0.073^{+0.023}_{-0.001}$	$0.124^{+0.035}_{-0}$
5	$0.072^{+0.044}_{-0.004}$	$0.100^{+0.069}_{-0.005}$	$0.166^{+0.109}_{-0.004}$

An ANN-based analysis for $\mu^+\mu^- \to l^+l^-\nu\nu\bar{\nu}\bar{\nu}$ at 30 TeV MuC makes expected constraints on dim-8 aQGCs that are 4 orders of magnitude stronger than those from the 13 TeV LHC.

aQGC: Tri-photon (AAA)

- aQGC in the $\mu^+\mu^- \to \gamma\gamma\gamma$ process

*Yang, Qin, Han, **Y-C G** & Li,* JHEP (2022) [2204.08195]

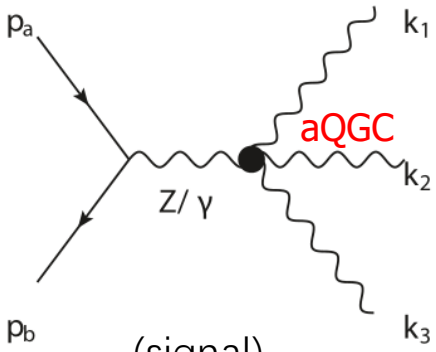

(signal)

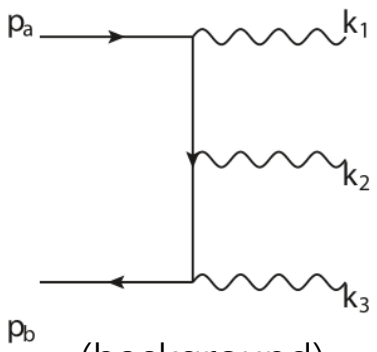

(background)

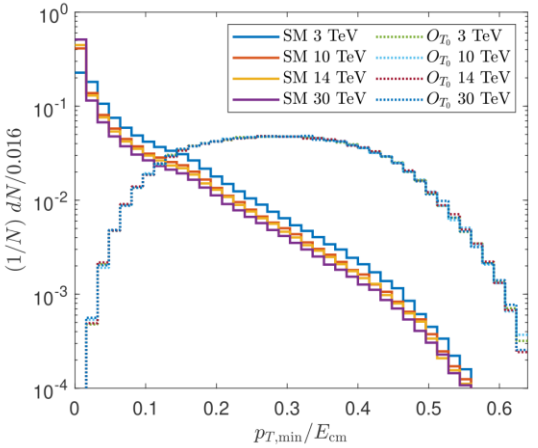

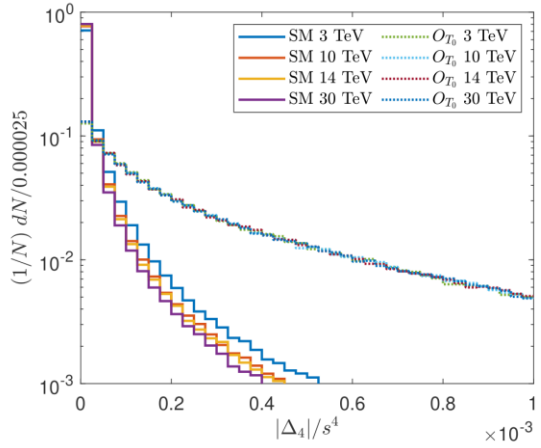

$$\Delta_4 = \frac{-1}{16}\left(2s_1(st_2(s_2+t_1)+(st_1-s_2t_2)(s_2-t_1))+(s(t_1-t_2)+s_2t_2)^2+s_1^2(s_2-t_1)^2\right)$$

$$O_{T_0} = \mathrm{Tr}\left[\widehat{W}_{\mu\nu}\widehat{W}^{\mu\nu}\right]\times\mathrm{Tr}\left[\widehat{W}_{\alpha\beta}\widehat{W}^{\alpha\beta}\right], \quad O_{T_1} = \mathrm{Tr}\left[\widehat{W}_{\alpha\nu}\widehat{W}^{\mu\beta}\right]\times\mathrm{Tr}\left[\widehat{W}_{\mu\beta}\widehat{W}^{\alpha\nu}\right]$$

$$O_{T_2} = \mathrm{Tr}\left[\widehat{W}_{\alpha\mu}\widehat{W}^{\mu\beta}\right]\times\mathrm{Tr}\left[\widehat{W}_{\beta\nu}\widehat{W}^{\nu\alpha}\right], \quad O_{T_5} = \mathrm{Tr}\left[\widehat{W}_{\mu\nu}\widehat{W}^{\mu\nu}\right]\times B_{\alpha\beta}B^{\alpha\beta},$$

$$O_{T_6} = \mathrm{Tr}\left[\widehat{W}_{\alpha\nu}\widehat{W}^{\mu\beta}\right]\times B_{\mu\beta}B^{\alpha\nu}, \quad O_{T_7} = \mathrm{Tr}\left[\widehat{W}_{\alpha\mu}\widehat{W}^{\mu\beta}\right]\times B_{\beta\nu}B^{\nu\alpha},$$

$$O_{T_8} = B_{\mu\nu}B^{\mu\nu}\times B_{\alpha\beta}B^{\alpha\beta}, \quad O_{T_9} = B_{\alpha\mu}B^{\mu\beta}\times B_{\beta\nu}B^{\nu\alpha},$$

$\sqrt{s}$		N_γ cut	$p_{T,\min}/E_{\rm cm} > 0.12$	$\lvert\Delta_4\rvert/s^4 > 3\times10^{-5}$	efficiency ϵ
3 TeV		4.495	1.085	0.686	0.115
10 TeV	SM	0.533	0.098	0.062	0.0877
14 TeV		0.289	0.050	0.031	0.0809
30 TeV		0.0718	0.0109	0.0069	0.0724
	O_{T_0}	0.0125	0.0117	0.0103	0.606
	O_{T_2}	0.0204	0.0193	0.0171	0.624
3 TeV	O_{T_5}	5.746	5.394	4.720	0.596
	O_{T_7}	4.706	4.443	3.935	0.613
	O_{T_8}	163.72	153.61	134.16	0.590
	O_{T_9}	189.36	178.86	158.14	0.606

Table 3. The cross-sections $\sigma_{\rm SM}$ and $\sigma_{O_{T_i}}$ (in unit of fb) and cut efficiencies after selection strategy. The results of aQGCs are obtained using the upper bound of the coefficients in table 1.

aQGC: Triboson (AAA)

aQGC in the $\mu^+\mu^- \to \gamma\gamma\gamma$ process

- The results show that the triphoton production of MuC is more sensitive to the $T_{8,9}$ operators
- For 3 TeV MuC with $\mathcal{L} = 1\ \mathrm{ab}^{-1}$, the expected constraints are 2 orders of magnitude stronger than 13 TeV LHC at 95% C.L.
- For 30 TeV MuC with $\mathcal{L} = 90\ \mathrm{ab}^{-1}$, the expected constraints would be about 6 orders of magnitude stronger than 13 TeV LHC.

Expected constraints on coefficients of $\mathcal{O}_{T_i}$ operators

	$\mathcal{S}_{\mathrm{stat}}$	3 TeV, $1\ \mathrm{ab}^{-1}$, $(10^{-2}\ \mathrm{TeV}^{-4})$	10 TeV, $10\ \mathrm{ab}^{-1}$, $(10^{-4}\ \mathrm{TeV}^{-4})$	14 TeV, $10\ \mathrm{ab}^{-1}$, $(10^{-4}\ \mathrm{TeV}^{-4})$	30 TeV, $10\ \mathrm{ab}^{-1}$, $(10^{-5}\ \mathrm{TeV}^{-4})$	14 TeV, $20\ \mathrm{ab}^{-1}$, $(10^{-5}\ \mathrm{TeV}^{-4})$	30 TeV, $90\ \mathrm{ab}^{-1}$, $(10^{-6}\ \mathrm{TeV}^{-4})$
$\frac{f_{T_0}(f_{T_1})}{\Lambda^4}$	2	$[-43.49, 14.47]$t	$[-35.72, 12.19]$	$[-10.14, 4.09]$	$[-6.19, 3.30]$	$[-92.11, 31.68]$	$[-43.99, 15.08]$
	3	$[-48, 57, 19.55]$	$[-39.98, 16.45]$	$[-11.50, 5.46]$	$[-7.21, 4.32]$	$[-103.1, 42.71]$	$[-49.24, 20.34]$
	5	$[-57.08, 28.06]$	$[-47.10, 23.57]$	$[-13.77, 7.73]$	$[-8.92, 6.03]$	$[-121.6, 61.15]$	$[-58.04, 29.13]$
$\frac{f_{T_2}}{\Lambda^4}$	2	$[-108.0, 22.66]$	$[-87.71, 19.31]$	$[-24.37, 6.62]$	$[-14.06, 5.65]$	$[-227.4, 49.89]$	$[-108.0, 23.88]$
	3	$[-116.9, 31.59]$	$[-95.25, 26.85]$	$[-26.85, 9.09]$	$[-16.00, 7.58]$	$[-246.9, 69.37]$	$[-117.3, 33.19]$
	5	$[-132.4, 47.06]$	$[-108.3, 39.87]$	$[-31.08, 13.32]$	$[-19.27, 10.86]$	$[-280.6, 103.0]$	$[-133.4, 49.27]$
$\frac{f_{T_5}(f_{T_6})}{\Lambda^4}$	2	$[-10.78, 2.61]$	$[-8.81, 2.22]$	$[-2.45, 0.758]$	$[-1.44, 0.638]$	$[-22.68, 5.76]$	$[-10.81, 2.75]$
	3	$[-11.78, 3.61]$	$[-9.65, 3.05]$	$[-2.72, 1.03]$	$[-1.65, 0.846]$	$[-24.86, 7.94]$	$[-11.85, 3.78]$
	5	$[-13.49, 5.32]$	$[-11.08, 4.49]$	$[-3.19, 1.50]$	$[-2.01, 1.20]$	$[-28.58, 11.66]$	$[-13.62, 5.56]$
$\frac{f_{T_7}}{\Lambda^4}$	2	$[-27.54, 3.98]$	$[-22.47, 3.38]$	$[-6.17, 1.17]$	$[-3.41, 1.04]$	$[-58.64, 8.67]$	$[-27.79, 4.16]$
	3	$[-29.22, 5.66]$	$[-23.89, 4.80]$	$[-6.64, 1.65]$	$[-3.79, 1.43]$	$[-62.29, 12.32]$	$[-29.53, 5.91]$
	5	$[-32.22, 8.66]$	$[-26.42, 7.32]$	$[-7.48, 2.48]$	$[-4.46, 2.10]$	$[-68.80, 18.83]$	$[-32.65, 9.02]$
$\frac{f_{T_8}}{\Lambda^4}$	2	$[-1.74, 0.42]$	$[-1.42, 0.355]$	$[-0.399, 0.121]$	$[-0.233, 0.102]$	$[-3.70, 0.916]$	$[-1.76, 0.439]$
	3	$[-1.90, 0.58]$	$[-1.56, 0.490]$	$[-0.443, 0.165]$	$[-0.267, 0.136]$	$[-4.05, 1.26]$	$[-1.92, 0.605]$
	5	$[-2.17, 0.86]$	$[-1.79, 0.721]$	$[-0.518, 0.239]$	$[-0.325, 0.193]$	$[-4.64, 1.86]$	$[-2.21, 0.890]$
$\frac{f_{T_9}}{\Lambda^4}$	2	$[-4.50, 0.63]$	$[-3.66, 0.538]$	$[-1.00, 0.188]$	$[-0.553, 0.167]$	$[-9.49, 1.39]$	$[-4.52, 0.664]$
	3	$[-4.77, 0.90]$	$[-3.89, 0.765]$	$[-1.07, 0.264]$	$[-0.615, 0.229]$	$[-10.08, 1.98]$	$[-4.80, 0.944]$
	5	$[-5.25, 1.38]$	$[-4.29, 1.17]$	$[-1.21, 0.399]$	$[-0.723, 0.337]$	$[-11.12, 3.02]$	$[-5.30, 1.44]$

aQGC: Triboson (AAA)

Search for aQGC by Machine Learning algorithms in $\mu^+\mu^- \to \gamma\gamma\gamma$

- K-Means *Zhang, Yang & **Y-C G**,* EPJC (2024) [2302.01274]

$$d(\vec{x},\vec{k}) = \left\|\vec{x}-\vec{k}\right\| = \left[\sum_{i=1}^{n}(x_i - k_i)^2\right]^{\frac{1}{2}}$$

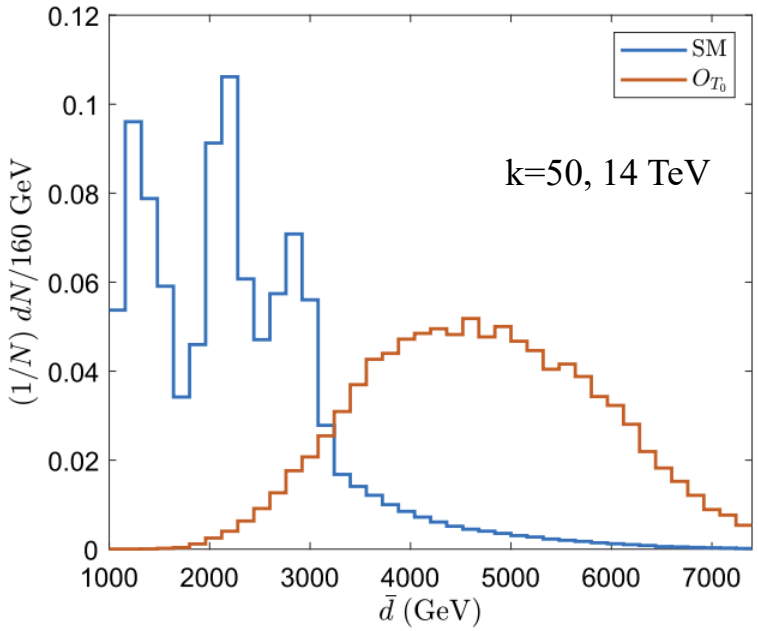

- Support Vector Machine (SVM)

*Zhang, **Y-C G** & Yang,* EPJC (2024) [2311.15280]

$$\sum_i W_i(p_i - \bar{p}_i)/d_i + b_{th} > y_{th}$$

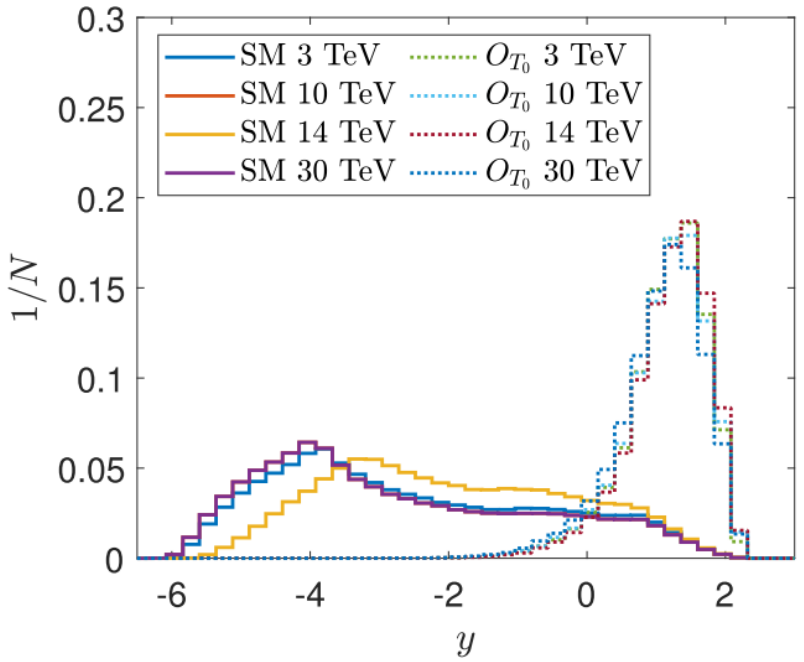

gQGC: Triboson (GGA)

Many discussions on EW QGC, less gluonic ones

- gQGC at LHC:

  $gg \to \gamma\gamma$ Ellis & Ge, PRL (2018) [1802.02416]

  $gg \to Z\gamma$ Ellis, Ge & K. Ma, JHEP (2022) [2112.06729]

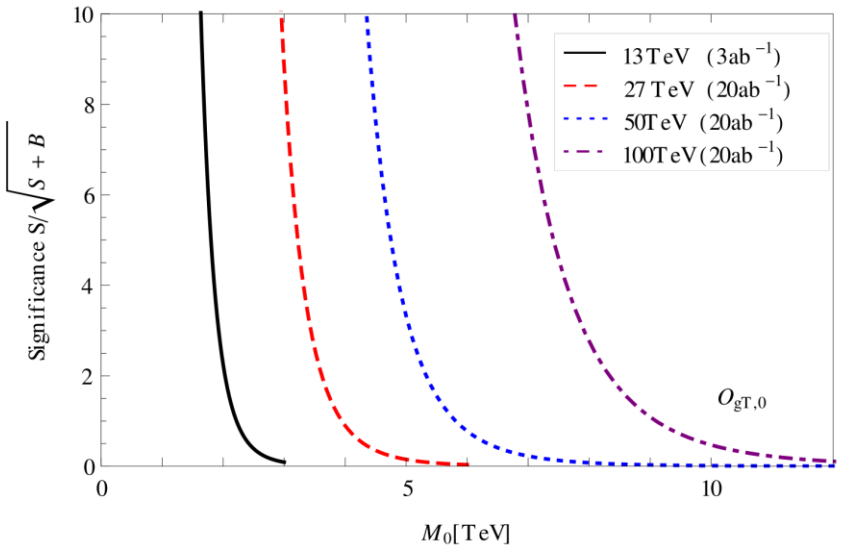

- gQGC at MuC: $\mu^+\mu^- \to gg\gamma$ ***Y-C G**, Di & Yang*, to be uploaded to arXiv

NP Signal:

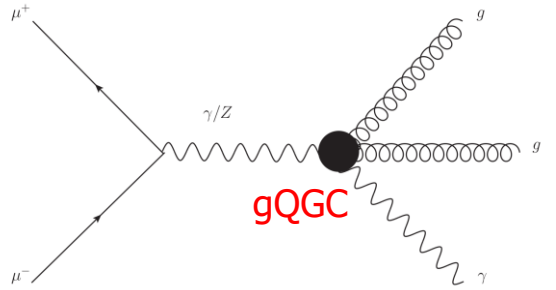

SM :

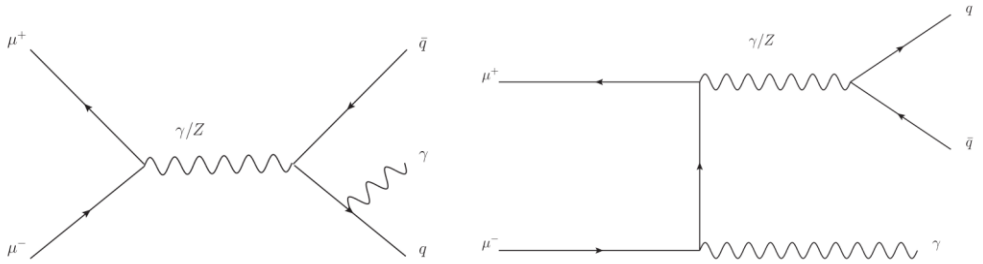

Most promising channel

- Dim-6 operators do not appear
- Clean signal
- No interference

gQGC: Triboson (GGA)

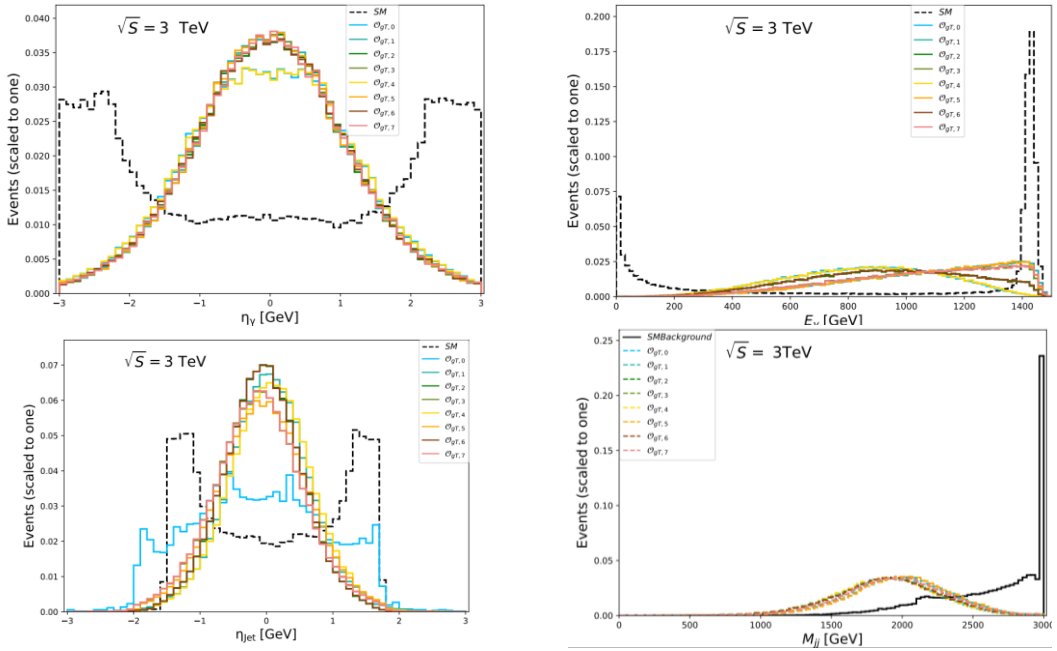

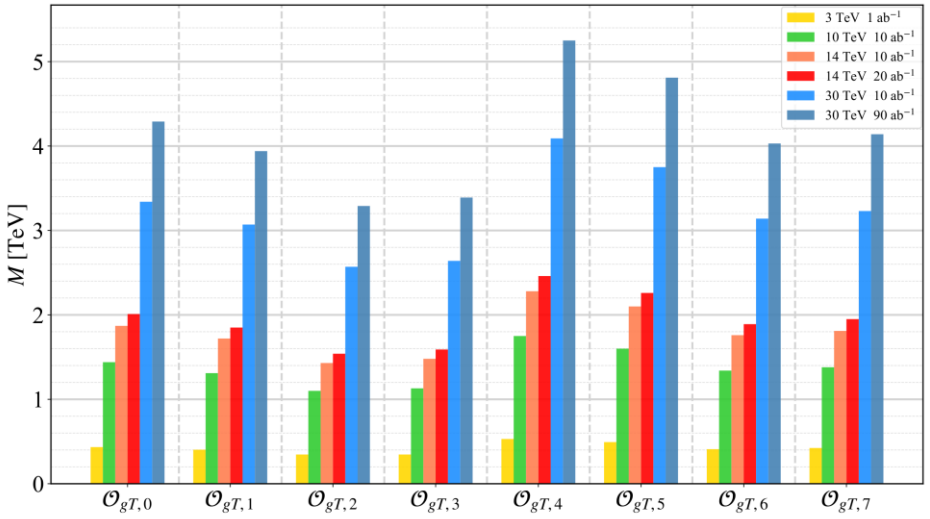

	$\mathcal{S}_{stat}$	3 TeV 1 ab^{-1}	10 TeV 10 ab^{-1}	14 TeV 10 ab^{-1}	14 TeV 20 ab^{-1}	30 TeV 10 ab^{-1}	30 TeV 90 ab^{-1}
$\lvert f_0\rvert$ (TeV^{-4})	2	< 1.76	< 0.0148	< 0.00515	< 0.00383	< 0.000500	< 0.000185
	3	< 2.48	< 0.0210	< 0.00745	< 0.00543	< 0.000746	< 0.000263
	5	< 3.94	< 0.0336	< 0.01215	< 0.00870	< 0.001230	< 0.000425
$\lvert f_1\rvert$ (TeV^{-4})	2	< 2.36	< 0.0212	< 0.00725	< 0.00540	< 0.000707	< 0.000261
	3	< 3.31	< 0.0300	< 0.01049	< 0.00764	< 0.001050	< 0.000372
	5	< 5.27	< 0.0480	< 0.01710	< 0.01219	< 0.001740	< 0.000599
$\lvert f_2\rvert$ (TeV^{-4})	2	< 5.00	< 0.0431	< 0.01499	< 0.0111	< 0.00145	< 0.000535
	3	< 7.01	< 0.0609	< 0.02169	< 0.0158	< 0.00215	< 0.000762
	5	< 11.1	< 0.0974	< 0.03529	< 0.0253	< 0.00357	< 0.001227
$\lvert f_3\rvert$ (TeV^{-4})	2	< 4.38	< 0.0390	< 0.0132	< 0.00984	< 0.00129	< 0.000479
	3	< 6.15	< 0.0551	< 0.0191	< 0.01339	< 0.00192	< 0.000682
	5	< 9.78	< 0.0881	< 0.0311	< 0.02229	< 0.00319	< 0.001098
$\lvert f_4\rvert$ (TeV^{-4})	2	< 0.79	< 0.00664	< 0.00232	< 0.00173	< 0.000224	< 0.000082
	3	< 1.11	< 0.00938	< 0.00336	< 0.00244	< 0.000333	< 0.000118
	5	< 1.76	< 0.01499	< 0.00548	< 0.00392	< 0.000550	< 0.000190
$\lvert f_5\rvert$ (TeV^{-4})	2	< 1.03	< 0.0095	< 0.00325	< 0.00242	< 0.000316	< 0.000117
	3	< 1.48	< 0.0134	< 0.00470	< 0.00342	< 0.000470	< 0.000166
	5	< 2.36	< 0.0215	< 0.00767	< 0.00549	< 0.000770	< 0.000268
$\lvert f_6\rvert$ (TeV^{-4})	2	< 2.24	< 0.0193	< 0.00664	< 0.00494	< 0.000648	< 0.000239
	3	< 3.14	< 0.0272	< 0.00961	< 0.00700	< 0.000963	< 0.000340
	5	< 5.00	< 0.0435	< 0.01567	< 0.01122	< 0.001590	< 0.000549
$\lvert f_7\rvert$ (TeV^{-4})	2	< 1.96	< 0.0175	< 0.00591	< 0.00440	< 0.000580	< 0.000214
	3	< 2.75	< 0.0247	< 0.00855	< 0.00623	< 0.000862	< 0.000305
	5	< 4.37	< 0.0394	< 0.01394	< 0.00999	< 0.001430	< 0.000491

Compared to 13 TeV LHC, 10 TeV MuC enhance the constraints by 25%, 30 TeV MuC would more than double the current limits on M.

Summary

- The MuC's nature as a lepton collider, coupled with its high energy and luminosity, facilitates both direct and indirect searches for new physics.
- Multi-boson physics at dimension-8 provide windows of opportunity for probing indirectly new physics BSM at the MuC.
- ML serves as a powerful tool in the search for new physics, continues to unlock breakthroughs of HEP.

Thank you !